Temporal dynamics of two-photon-pumped amplified spontaneous emission in slab organic crystals

Hong-Hua Fang,[1] Qi-Dai Chen,[1] Ran Ding,[1] Jie Yang,[1] Yu-Guang Ma,[2] Hai-Yu Wang,[1] Bing-Rong Gao,[1] Jing Feng,[1,4] and Hong-Bo Sun[1,3,5]

[1]*State Key Laboratory on Integrated Optoelectronics, College of Electronic Science and Engineering, Jilin University, 2699 Qianjin Street, Changchun 130012, China*

[2]*State Key Laboratory of Supramolecular Structures and Materials, College of Chemistry, Jilin University, 2699 Qianjin Street, Changchun 130012, China*

[3]*College of Physics, Jilin University, 119 Jiefang Road, Changchun 130023, China*

[4]*e-mail: jingfeng@jlu.edu.cn*

[5]*e-mail: hbsun@jlu.edu.cn*

Received April 26, 2010; revised June 29, 2010; accepted July 2, 2010; posted July 8, 2010 (Doc. ID 127590); published July 22, 2010

We have studied the ultrafast dynamics of two-photon-pumped amplified spontaneous emission (ASE) from a single crystal by the time-resolved fluorescence upconversion technique. With the increase of two-photon pump intensities, the emission decay time is dramatically shortened by 30 times (from 3 ns to ~87 ps), and the energy migration rate is acutely enhanced when ASE occurs. The stripe length is also found to play an important role in the formation of the ASE. Meanwhile, the gain coefficient is evaluated to be 15 cm^{-1} for 560 nm at an excitation intensity of 2.3 $mJ/pulse/cm^2$ by the variable stripe length technique.

OCIS codes: 160.4890, 140.3613, 190.4180, 190.7110.

Organic crystals have attracted much interest because of their unique properties for applications in electronics, photonics, and nonlinear optics, such as in the organic field effect transistor [1], solid-state laser [2,3], and terahertz generation [4]. They generally offer the highest optical and electronic performance of any solid-state organic materials and typically outperform their polycrystalline counterparts [5,6]. The light shows preferential propagation directions [7] and well-defined polarization states [8]. Moreover, organic crystals exhibit a high degree of spectral tunability, large stimulated emission cross sections (high gain coefficient), and low propogation loss [9], which is very important for laser applications. Despite the challenge in the growth of quality compared with other materials, such as thin films [10], organic crystals still show great potential for use in an upconversion laser device.

The recent demonstration of two-photon-pumped (TPP) stimulated emission in the organic crystals has stirred widespread attention for its potential compact solid-state upconversion laser application [8,11–14]. Different with one-photon absorption, two-photon absorption is a nonlinear process, where two photons are absorbed simultaneously through a virtual state. Then the materials can be pumped at a longer wavelength, which is beneficial for increasing the lifetime and photostability of the materials. In a previous study, we observed TPP amplified spontaneous emission (ASE) in DBASDMB crystals [13], realized low threshold TPP ASE in Ph-TPA2 crystals [12], and achieved high polarization and directional upconverted emission in an uniaxial crystal [8]. However, these factors are not enough for many applications in the time domain, which need temporal information. The physical insight of the temporal properties, which are untouched, may help not only to understand the process of the formation of the TPP ASE but also to better exploit the potentialities of organic crystals and to improve pulsed laser performances.

In this Letter, we have tried to understand TPP ultrafast transient stimulated emission dynamics by the time-resolved fluorescence upconversion technique with 200 fs resolution, from the slab crystals of cyano-substituted oligo (*p*-phenylenevinylene), which were demonstrated to emit an upconverted yellow–green emission (around 560 nm) with high polarization and direction under two-photon excitation (800 nm) [8]. For the temporal evolution of the transient process, an isolated single crystal about 2.5 mm long and 0.5 mm wide is selected in the experiment and probed by subsequent upconversion of the emission output, as shown in Fig. 1. The pulse from the Ti:sapphire regenerative amplifier with laser pulse of 800 nm, ~100 fs optical pulse duration, and 1 kHz repetition rate is split into two parts. One is focused onto the crystal sample; the other is sent into an optical delay line and serves as the gate pulse. The generated sum frequency light was then collimated and focused into the entrance slit of a 300 mm monochromator, spectrally resolved, and detected by a photomultiplier tube. In the setup, the pulse energy of the

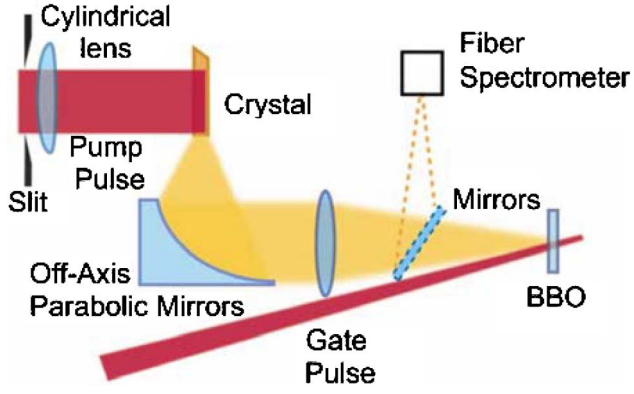

Fig. 1. (Color online) Schematic diagram of the gated frequency upconversion technique for the temporal behavior of TPP ASE.

pump laser was controlled using neutral density filters. An adjustable slit and a cylindrical lens were used in order to shape the beam into a narrow stripe (~0.5 mm width) with a continuously varied length on the crystal. The emission light from the crystal was collected by an off-axis parabolic mirror and focused on the beta-barium-borate (BBO) crystal. In this configuration, fluorescent light is collected in the direction parallel to the long axes of the crystal. Then the emission dynamics can be directly observed from the tip of the crystals. A fiber spectrometer was introduced to monitor the time-integrated emission spectra from the crystal.

Figure 2(a) shows the normalized temporal profiles for the TPA-induced stimulated emission observed from one tip of the crystal excited at different intensities, where the monitor wavelength corresponded to the peak position of time-integrated spectra, as is shown in the Fig. 2(b). Under the excitation power density of lower than the onset value of the stimulated emission, the spectra are very broad (FWHM = 68 nm) and are dominated by regular photoluminescence (PL), as marked with "A" in Fig. 2(b). The emission shows a very slow decay with a time constant of about 3 ns [line A in Fig. 2(a)]. When the excitation intensity reaches the onset value of the ASE threshold (1.5 mJ/pulse/cm^2), the spectra begin to collapse to be 44 nm (line B) centered around 566 nm. In the meantime, a new component appeared with the increased pump intensity, which is assigned as stimulated emission. Both the temporal dynamics and time-integrated emission show a clear threshold as the pump intensities increase. We note that this "bump" component is faster than the normal PL. When the intensity is further increased, this component becomes more apparent and faster; the pulse duration time becomes shorter (down to 87 ps), and the peak of the spectra is more blueshifted.

The transient dynamics profiles obtained at the different wavelengths will help map out the ASE process more

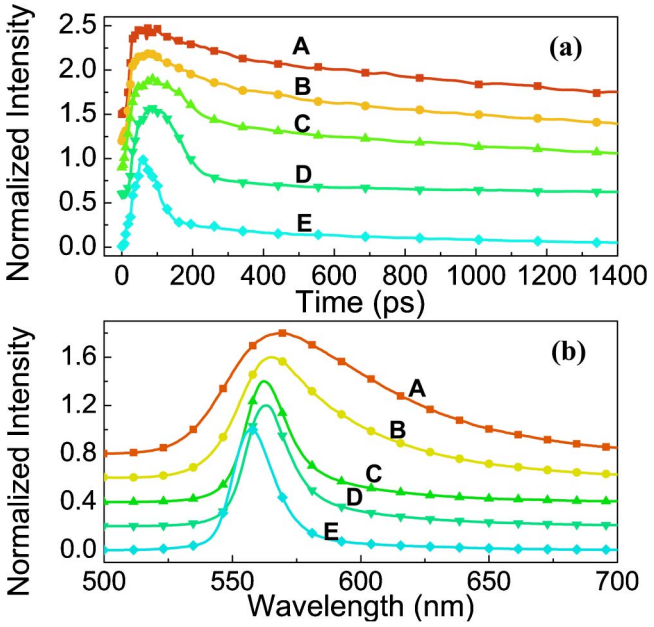

Fig. 2. (Color online) (a) Transient emission at different pump intensities, A < B < C < D < E. (b) Integrated emission from the crystals recorded at corresponding excitation intensities.

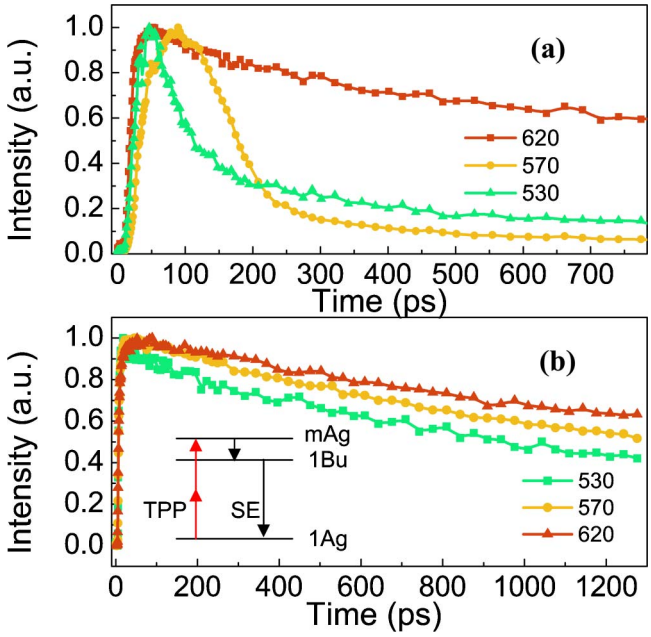

Fig. 3. (Color online) (a) Transient emission at the pump intensities above the ASE threshold. (b) Transient emission at the pump intensities below the ASE threshold: SE, stimulated emission.

clearly. Figures 3(a) and 3(b) show the dynamics pumped at 3 mJ/pulse/cm^2 (slightly above the threshold) and 0.75 mJ/pulse/cm^2 (below the threshold), respectively, for three wavelengths, 530 nm, 570 nm, and 620 nm. Under low-intensity excitation, the three emission wavelengths all show slow decay characteristic but slightly faster for the short wavelength, suggesting energy migration occurs within the exciton distribution. While the condition is different upon the pump intensity increase, decay at the short wavelength (530 nm) becomes extremely short within a time of less than 100 ps. Although the decay for 570 nm also shows a very fast rate at high intensity, we can find that a slow rise appears. The relatively long rise time for the 570 nm wavelength is comparable to the fast decay time in 530 nm, suggesting that the energy migration within the excitonic states distribution plays an important role in the formation of ASE [15]. The energy migration rate strongly depends on the pump intensity. The "bump" in the 570 nm wavelength represented the stimulated emission, whose FWHM become very narrow. The TPA ASE dynamics may be described analogous to the situation of single-photon pumping [16] as the following. Upon pumping the excited state, the population decays initially. After some time the strongly nonlinear photon amplification process leads to the generation of the emission pulse. However, the population inversion is not achieved immediately after the pump, while the formation of the stimulated emission requires a certain time (energy migration within the excitonic states distribution). After the formation of the population inversion, the high density of the excited states is rapidly reduced by the stimulated emission process. The ASE process stops as soon as the population inversion is terminated.

The emission dynamics was further investigated under different stripe lengths at the pump intensity of

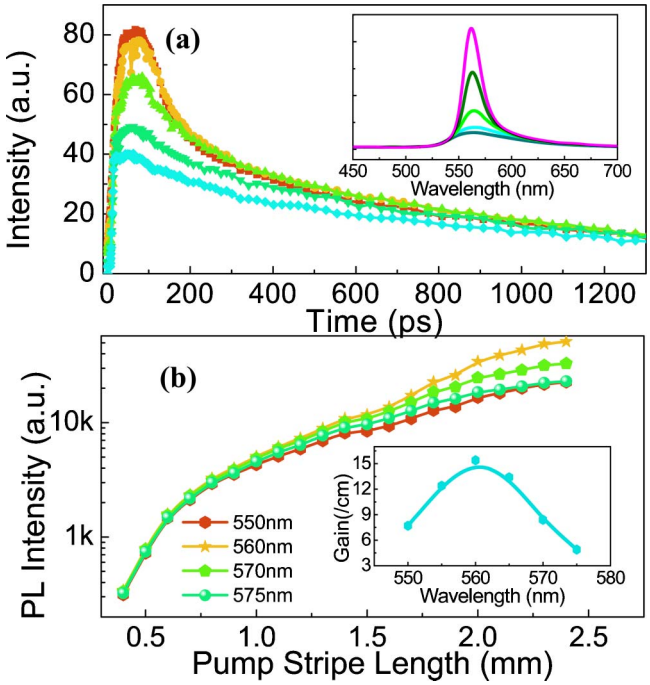

Fig. 4. (Color online) (a) Emission dynamics of the crystal at 560 nm for different stripe lengths at pump intensity of 2.3 mJ/pulse/cm^2 and corresponding time-integrated emission (inset). (b) PL intensity versus stripe length and calculated gain coefficient for different wavelengths (inset).

2.3 mJ/pulse/cm^2, and we monitored the corresponding time-integrated spectra and temporal features [Fig. 4(a)]. It is seen that the PL intensity increases as the stripe length increases; the overall emission is much more intense at a long stripe length. More important, the shape of the spectrum changed dramatically; the FWHM changed from 62 nm to 18 nm. On the other hand, the decay time also varies among the different stripe length. A new component appeared with the increased stripe length, which is very similar to the condition mentioned above. This directly suggests that the waveguide propagation (photons confined in the crystal and propagated in preferential directions) effect plays an extremely important role in the ASE process.

The emission intensity versus the pump stripe length for different wavelengths was plotted in Fig. 4(b). A superlinear increase in the intensity with the excitation length was clearly observed, and the data in Fig. 4(b) were fitted (in the low output intensity regime) with the following relationship [17]:

$$I(\lambda) = \frac{AI_p}{g(\lambda)}(e^{g(\lambda)l} - 1), \quad (1)$$

where A is a constant related to the cross section for spontaneous emission, I_p is the pump intensity, g is the net gain coefficient, and l is the length of the pumped stripe. The g at the wavelength of 560 nm was deduced to be 15 cm^{-1} at 2.3 mJ/pulse/cm^2. Moreover, the loss coefficient was evaluated, where the length of the pump stripe is kept constant and moves away from the edges of the crystal, and then the edge emission was detected. Then the intensity data versus the unpumped length can be obtained. The crystal shows a low loss coefficient of less than 6 cm^{-1} at 560 nm, which is one of the lowest values.

In conclusion, we have used the gated frequency upconversion technique to fully resolve the temporal behavior of TPP ASE from slab organic crystal. By direct measurement of the emission kinetics, we observed fast emission with a pulse duration FWHM = 87 ps without a feedback resonator. The ASE temporal evolutions are not only highly dependent on the pump intensities, but also the stripe length, suggesting the important role of the waveguide effect on the formation of TPP ASE. We also found that the energy migration rate becomes much higher at a high intensity. Finally, high gain coefficient under the two-photon pumping condition was achieved, showing great potential for the upconversion laser.

This work was financially supported by the National Natural Science Foundation of China (NSFC) (grants 90923037, 60525412, and 60877019).

References

1. A. L. Briseno, R. J. Tseng, M. M. Ling, E. H. L. Falcao, Y. Yang, F. Wudl, and Z. N. Bao, Adv. Mater. **18**, 2320 (2006).
2. M. Ichikawa, R. Hibino, M. Inoue, T. Haritani, S. Hotta, K. Araki, T. Koyama, and Y. Taniguchi, Adv. Mater. **17**, 2073 (2005).
3. H. H. Fang, Q. D. Chen, J. Yang, L. Wang, Y. Jiang, H. Xia, J. Feng, Y. G. Ma, H. Y. Wang, and H. B. Sun, Appl. Phys. Lett. **96**, 103508 (2010).
4. O. P. Kwon, S. J. Kwon, M. Jazbinsek, F. D. J. Brunner, J. I. Seo, C. Hunziker, A. Schneider, H. Yun, Y. S. Lee, and P. Gunter, Adv. Funct. Mater. **18**, 3242 (2008).
5. C. Reese, M. E. Roberts, S. R. Parkin, and Z. A. Bao, Appl. Phys. Lett. **94**, 202101 (2009).
6. Y. P. Li, F. Z. Shen, H. Wang, F. He, Z. Q. Xie, H. Y. Zhang, Z. M. Wang, L. L. Liu, F. Li, M. Hanif, L. Ye, and Y. G. Ma, Chem. Mater. **20**, 7312 (2008).
7. H. Yanagi, T. Ohara, and T. Morikawa, Adv. Mater. **13**, 1452 (2001).
8. H. H. Fang, Q. D. Chen, J. Yang, H. Xia, Y. G. Ma, H. Y. Wang, and H. B. Sun, Opt. Lett. **35**, 441 (2010).
9. W. J. Xie, Y. P. Li, F. Li, F. Z. Shen, and Y. G. Ma, Appl. Phys. Lett. **90**, 3 (2007).
10. B. Ullrich and R. Schroeder, Semicond. Sci. Technol. **16**, L37 (2001).
11. L. J. Zhao, J. J. Xu, G. Y. Zhang, X. H. Bu, and M. Shionoya, Opt. Lett. **24**, 1793 (1999).
12. Q. D. Chen, H. H. Fang, B. Xu, J. Yang, H. Xia, F. P. Chen, W. J. Tian, and H. B. Sun, Appl. Phys. Lett. **94**, 201113 (2009).
13. H. Xia, J. Yang, H. H. Fang, Q. D. Chen, H. Y. Wang, X. Q. Yu, Y. G. Ma, M. H. Jiang, and H. B. Sun, Chem. Phys. Chem. **11**, 1871 (2010).
14. F. Gao, Q. Liao, Z. Z. Xu, Y. H. Yue, Q. Wang, H. L. Zhang, and H. B. Fu, Angew. Chem. Int. Ed. **49**, 732 (2010).
15. C. W. Lee, K. S. Wong, J. D. Huang, S. V. Frolov, and Z. V. Vardeny, Chem. Phys. Lett. **314**, 564 (1999).
16. M. Zavelani-Rossi, S. Perissinotto, G. Lanzani, M. Salerno, and G. Gigli, Appl. Phys. Lett. **89**, 181105 (2006).
17. M. D. McGehee, R. Gupta, S. Veenstra, E. K. Miller, M. A. Díaz-García, and A. J. Heeger, Phys. Rev. B **58**, 7035 (1998).